

PREPARED FOR SUBMISSION TO JHEP

# Spontaneous scale symmetry breaking at high temperature

---

**Z. Lalak and P. Michalak**

*Institute of Theoretical Physics, Faculty of Physics,  
University of Warsaw, ul. Pasteura 5, 02-093 Warsaw, Poland*

*E-mail:* [z.lalak@uw.edu.pl](mailto:z.lalak@uw.edu.pl), [pmichalak@fuw.edu.pl](mailto:pmichalak@fuw.edu.pl)

**ABSTRACT:** We consider a scale symmetric extension of the Standard Model Higgs scalar sector. The new sector, dilaton, is responsible for the generation of mass scales and may have geometric origin in the Weyl gravity  $\tilde{R}^2$  term. We show how temperature as a mass scale breaks scale symmetry explicitly and through a nonvanishing thermal vev. In addition we demonstrate that cosmological evolution of the dilaton-Higgs system can lead to late time mass scales, which agree with the Standard Model.

---

## Contents

<b>1</b>	<b>Introduction</b>	<b>1</b>
<b>2</b>	<b>Theoretical motivation:</b>	<b>3</b>
2.1	Weyl gravity	3
2.2	Stueckelberg mechanism for Weyl vector field	4
2.2.1	Matter fields	5
<b>3</b>	<b>Scale symmetric potential</b>	<b>5</b>
3.1	Higgs potential parameters and Planck mass:	6
<b>4</b>	<b>Temperature corrections</b>	<b>7</b>
4.1	Quantum Field Theory at finite temperature:	7
4.2	Symmetry breaking at high temperature	9
4.2.1	Numerical analysis	10
4.3	Thermal equilibrium	12
<b>5</b>	<b>Time evolution of the fields</b>	<b>14</b>
5.1	Zero temperature	14
5.2	Non-zero temperature	16
5.3	$T = 0$ vs $T \neq 0$	18
5.4	Electroweak Symmetry Breaking	20
<b>6</b>	<b>Additional scalars</b>	<b>20</b>
<b>7</b>	<b>Summary and discussion</b>	<b>21</b>

---

## 1 Introduction

The Standard Model (SM) has a number of yet unresolved problems that may indicate that it is a part of a larger and more fundamental theory. This theory would explain the gaps in the current models. One such problem is the so-called hierarchy problem. Despite the fact that SM is a renormalizable theory, to keep the Higgs mass hierarchically lower than the Planck mass scale  $M_P$  in the presence of quantum corrections, as measured in experiments, one needs to arrange for very precise cancelations between a priori unrelated contributions to the effective potential of the scalar sector. This problem can be avoided in theory with the mechanism forcing  $m_H = 0$ , i.e. in the model with scale symmetry or conformal symmetry. However, nonzero Higgs mass must somehow be generated in these types of models. Mechanism generating  $m_H$  may be associated with an explicit violation of scale symmetry, e.g. by a quantum anomaly, or with spontaneous breaking of scale

symmetry. For consistency, such a theory needs to be coupled with a version of gravity, which, to some extent, respects the scale symmetry. The problem of explaining the Higgs mass hierarchically smaller than the Planck scale is one of the greatest challenges of modern theory of fundamental interactions, therefore all attempts to solve it are in the center of attention of researchers.

There are many proposals and specific models of scale symmetric Higgs scalar sector extended by scalar singlet [23–37]. Usually, such models are coupled to Einstein, or Brans-Dicke, gravity. What seems to be an attractive alternative solution is to use a natural extension of Riemannian geometry - the Weyl geometry [6–13], which avoids many problems encountered in Einstein formulation of gravity non-minimally coupled to scalar fields [13]. Using Weyl geometry, the new scalar sector, dilaton  $\phi_0$ , is not added *ad hoc* to the Lagrangian, but has a geometric origin. Its vev generates all mass scales in the theory, so  $M_P$  and  $m_H$  arise naturally.

Scale symmetry does not have to be broken by dimensional regularization  $\mu = \text{const}$  or dimensionfull cutoff  $\Lambda$ . As indicated in previous proposals [1–5, 14], renormalization scale can be a function of dilaton  $\mu = \mu(\phi_0)$ . This way, the scale symmetry is preserved at the quantum level and after spontaneous scale symmetry breaking (SSSB), when dilaton acquires a vev  $\langle\phi_0\rangle$ , the subtraction scale  $\mu(\langle\phi_0\rangle)$  is generated dynamically. Therefore, due to SSB another important mass scale is generated, not only  $M_P$  and  $m_H$ . Preserving scale symmetry with  $\mu = \mu(\phi_0)$  leads to new finite quantum corrections absent in standard Coleman-Weinberg results [15]. For a discussion of quantum corrections in this case, one should consult earlier work reported in [1–5, 14].

What has not been analyzed yet are thermal corrections to classically scale invariant potential for Higgs scalar sector extended with dilaton. Such a study seems natural since if one wants to examine the cosmological evolution of the model, adding temperature corrections allows for the fact that the Universe is hot during expansion. Since the temperature  $T$  is an explicit mass scale, it explicitly breaks the scale symmetry. Temperature corrections to the Higgs sector only, display electroweak symmetry restoration at high temperature [18]. Namely, Higgs expectation value is driven to zero and electroweak symmetry breaking (EWSB) occurs only after the system cools down. The shape of the thermally corrected potential for the Higgs suggests that EWSB is a second order, or weakly first order, phase-transition. The case may be different though if one adds additional new scalar singlet, dilaton. We analyze the results of time evolution of the fields in hot Universe to show the nature of EWSB in our model and to simulate the dynamical mass scale generation when dilaton settles at its final value  $\langle\phi_0\rangle$ .

The paper is organized as follows: in Section 2 we describe basic properties of Weyl conformal geometry by itself and coupled to matter fields. Section 3 provides analysis of classically scale symmetric potential used in the presented model and available parameter space. Section 4 includes short description of finite temperature corrections and their application to considered theory. We show how temperature as a mass scale breaks scale symmetry explicitly and how it affects the potential changing the ground state. In Section 5 we present numerical simulations of time evolution of fields  $\phi_0$  and  $\phi_1$  in both zero temperature case and in hot Universe. We show that one can reasonably choose initial

conditions in such a way that one obtains at late times of the evolution a realistic model fitting our present knowledge.

## 2 Theoretical motivation:

### 2.1 Weyl gravity

In the following section, we will show the basic properties of Weyl's conformal geometry [6–13] and its application to construct an action invariant under conformal Weyl transformations. Discussion in this section will lead us to very important conclusion: Einstein gravity is a low energy limit of Weyl gravity.

The main difference between Riemannian gravity and Weyl gravity is the presence of Weyl gauge vector field  $\omega_\mu$ . Weyl quantities will be denoted with a tilde and Riemannian ones stay without a tilde. Connection  $\tilde{\Gamma}_{\mu\nu}^\rho$  takes the form:

$$\tilde{\Gamma}_{\mu\nu}^\rho = \Gamma_{\mu\nu}^\rho + \frac{q}{2} [\delta_\mu^\rho \omega_\nu + \delta_\nu^\rho \omega_\mu - g_{\mu\nu} \omega^\rho], \quad (2.1)$$

where  $q$  is the coupling of  $\omega_\mu$  to the scalar field  $\phi$  from the Weyl covariant derivative:

$$\tilde{D}_\mu \phi = \left( \partial_\mu - \frac{q}{2} \omega_\mu \right) \phi. \quad (2.2)$$

The system is torsion free i.e.  $\tilde{\Gamma}_{\mu\nu}^\rho = \tilde{\Gamma}_{\nu\mu}^\rho$ . It is easy to see, that if we take the limit  $\omega_\mu \rightarrow 0$ , Riemannian geometry is recovered and  $\tilde{\Gamma}_{\mu\nu}^\rho \rightarrow \Gamma_{\mu\nu}^\rho$ . The Weyl covariant derivative of the metric, in contrast to Riemannian one, is different from zero:

$$\tilde{\nabla}_\mu g_{\alpha\beta} = -q \omega_\mu g_{\alpha\beta}. \quad (2.3)$$

This is why in Weyl geometry parallel transport of a vector along a closed curve changes not only its direction (as in Einstein gravity case) but also its length. The Weyl curvature scalar takes form:

$$\tilde{R} = R - 3q D_\mu \omega^\mu - \frac{3}{2} q^2 \omega_\mu \omega^\mu, \quad (2.4)$$

where  $D_\mu$  is the Riemannian covariant derivative with the Levi-Civita connection  $\Gamma_{\mu\nu}^\rho$ . Weyl field  $\omega_\mu$  is abelian, thus the field strength tensor  $\tilde{F}_{\mu\nu}$  for  $\omega_\mu$  is equal to the Riemannian one:

$$\tilde{F}_{\mu\nu} = \tilde{D}_\mu \omega_\nu - \tilde{D}_\nu \omega_\mu = \partial_\mu \omega_\nu - \partial_\nu \omega_\mu = F_{\mu\nu}, \quad (2.5)$$

where  $\tilde{D}_\mu$  is covariant derivative with connection  $\tilde{\Gamma}_{\mu\nu}^\rho$ .

Weyl gauge invariance of the action is manifested by invariance under conformal transformations of the metric  $g_{\mu\nu}$ , scalar field  $\phi$  and Weyl vector field  $\omega_\mu$ :

$$\begin{aligned} g_{\mu\nu} &\longrightarrow g'_{\mu\nu} = \Omega^2 g_{\mu\nu}, \\ \phi &\longrightarrow \phi' = \frac{\phi}{\sqrt{\Omega}}, \\ \omega_\mu &\longrightarrow \omega'_\mu = \omega_\mu - \frac{1}{q} \partial_\mu \ln \Omega, \end{aligned} \quad (2.6)$$

where  $\Omega$  is dimensionless parameter. Then  $\sqrt{g'} = \Omega^4 \sqrt{g}$ ,  $\tilde{R}' = \Omega^{-2} \tilde{R}$  and  $\tilde{F}'_{\mu\nu} = \tilde{F}_{\mu\nu}$ .

## 2.2 Stueckelberg mechanism for Weyl vector field

Now we are going to consider the theory containing only Weyl quadratic gravity and vector field  $\omega_\mu$  in the absence of matter. The original Lagrangian for Weyl quadratic gravity invariant under (2.6) can be of the form:

$$\frac{\mathcal{L}_W}{\sqrt{g}} = \frac{\xi_0}{4!} \tilde{R}^2 - \frac{1}{4} g^{\mu\nu} g^{\rho\sigma} \tilde{F}_{\mu\rho} \tilde{F}_{\nu\sigma}, \quad (2.7)$$

where  $\xi_0 > 0$ . The  $\tilde{R}^2$  term propagates additional scalar state, so we can substitute:

$$\tilde{R}^2 \rightarrow -2\phi_0^2 \tilde{R} - \phi_0^4. \quad (2.8)$$

Equation of motion for  $\phi_0$  gives  $\phi_0^2 = -\tilde{R}$ , thus the Weyl quadratic gravity term is recovered and we can consider an equivalent Lagrangian of the form:

$$\frac{\mathcal{L}_W}{\sqrt{g}} = -\frac{\xi_0}{12} \phi_0^2 \tilde{R} - \frac{1}{4} g^{\mu\nu} g^{\rho\sigma} \tilde{F}_{\mu\rho} \tilde{F}_{\nu\sigma} - \frac{\xi_0}{4!} \phi_0^4. \quad (2.9)$$

In the above Lagrangian we have one massless scalar field  $\phi_0$  and one massless vector field  $\omega_\mu$  present in  $\tilde{R}$  and  $\tilde{F}_{\mu\nu}$  terms. Now, we apply (2.6) transformations to it with  $\Omega = \xi_0 \phi_0^2 / 6M^2$ :

$$\phi_0^2 = \frac{\phi_0^2}{\Omega} = \frac{6M^2}{\xi_0}, \quad \tilde{R}' = R' - \frac{3}{2} q^2 \omega'_\mu \omega'^\mu + (\text{total deriv.}) \quad (2.10)$$

Neglecting the total derivative term, we obtain:

$$\frac{\mathcal{L}'_W}{\sqrt{g'}} = -\frac{1}{2} M^2 R' + \frac{3}{4} q^2 M^2 \omega'_\mu \omega'^\mu - \frac{1}{4} \tilde{F}'_{\mu\nu} \tilde{F}'^{\mu\nu} - \frac{3}{2\xi_0} M^4, \quad (2.11)$$

where  $R'$  is the Riemannian curvature scalar after transformation (2.6). Weyl vector field became massive via the Stueckelberg mechanism  $m_\omega^2 = \frac{3}{4} q^2 M^2$ . Usually  $M$  is chosen to  $M_{Planck}$ . So Planck mass scale is naturally generated after breaking of the Weyl conformal symmetry (via Stueckelberg mechanism). This phenomena, impossible in Riemannian gravity, can give the solution to the hierarchy problem and originates mass scales in physics.

The Lagrangian (2.11) is the Einstein-Proca action for Weyl gauge field. It is worth observing that the number of degrees of freedom is conserved. We had massless vector and a scalar field, which gives 3 d.o.f. and after the gauge symmetry transformation we have only one vector massive field, still 3 d.o.f. This is happening because the vector field  $\omega_\mu$  has "eaten" dilaton mode  $\phi_0$  (actually the real dilaton is  $\ln \phi_0^2$  with shift symmetry:  $\ln \phi_0^2 \rightarrow \ln \phi_0^2 - \ln \Omega$ , but we will refer to  $\phi_0$  field as dilaton in this work, since it will remain massless). Without  $\omega_\mu$  conservation of d.o.f. wouldn't be possible. In  $\mathcal{L}_W$  there is also a positive cosmological constant term. For a coupling  $q$  not too small, the mass of the Weyl vector field is close to the Planck's mass. Below this scale, the  $\omega_\mu$  decouples and the whole theory becomes Riemannian. So Einstein gravity can be considered as the low energy limit of Weyl gravity.

### 2.2.1 Matter fields

In this paper, we are considering a scale symmetric extension of the Standard Model Higgs scalar sector. Therefore, in addition to Lagrangian (2.9), we want to consider a more general case. Let us denote  $\phi_1$  as a Higgs neutral component. Lagrangian invariant under (2.6) is:

$$\frac{\mathcal{L}}{\sqrt{g}} = -\frac{1}{12}(\xi_0\phi_0^2 + \xi_1\phi_1^2)\tilde{R} - \frac{1}{4}\tilde{F}_{\mu\nu}\tilde{F}^{\mu\nu} + \frac{1}{2}\tilde{D}_\mu\phi_0\tilde{D}^\mu\phi_0 + \frac{1}{2}\tilde{D}_\mu\phi_1\tilde{D}^\mu\phi_1 - V(\phi_0, \phi_1), \quad (2.12)$$

where we added kinetic terms for  $\phi_i$  fields with covariant derivative (2.2) and  $V(\phi_0, \phi_1)$  is scale symmetric potential, which includes possible interactions between  $\phi_i$  fields and will be specified later.

Now, we can apply the transformations (2.6) to (2.12) with:

$$\Omega = \frac{\xi_0\phi_0^2 + \xi_1\phi_1^2}{6M^2}. \quad (2.13)$$

One gets:

$$\frac{\mathcal{L}'}{\sqrt{g'}} = -\frac{1}{2}M^2R' + \frac{3}{4}q^2M^2\omega'_\mu\omega'^\mu - \frac{1}{4}\tilde{F}'_{\mu\nu}\tilde{F}'^{\mu\nu} + \frac{1}{2}\tilde{D}'_\mu\phi'_0\tilde{D}'^\mu\phi'_0 + \frac{1}{2}\tilde{D}'_\mu\phi'_1\tilde{D}'^\mu\phi'_1 - V'(\phi'_0, \phi'_1), \quad (2.14)$$

which again is the Einstein-Proca action with Weyl gauge field and two  $\phi_0, \phi_1$  scalars. Initially massless  $\omega_\mu$  field, acquires mass  $m_\omega^2 = \frac{3}{4}q^2M^2$  and for energies below that scale, can be considered as decoupled and the whole theory becomes Riemannian.

The above discussion shows that after spontaneous scale symmetry breaking, i.e. when scalar fields  $\phi_i$  acquire their vevs, so that

$$\frac{1}{6}(\xi_0\langle\phi_0^2\rangle + \xi_1\langle\phi_1^2\rangle) = M^2, \quad (2.15)$$

the mass scales are generated. The question is: how does this happen? What are the values of  $\langle\phi_i\rangle$  and how to obtain Standard Model Higgs sector from this theory? In the next sections we will present an answer to those questions, properties of the scale symmetric potential  $V(\phi_0, \phi_1)$  and evolution of  $\phi_i$  fields coupled to gravity. We will show that in this model, gravitational evolution of the system can lead to a final state, which agrees with SM parameters, that are determined in the experiments.

## 3 Scale symmetric potential

Let us consider a low-energy limit of Weyl gravity with Higgs scalar sector, so the  $\omega_\mu$  field is heavy and may be omitted in Lagrangian. We have:

$$\frac{\mathcal{L}}{\sqrt{g}} = -\frac{1}{12}(\xi_0\phi_0^2 + \xi_1\phi_1^2)R + \frac{1}{2}\partial_\mu\phi_0\partial^\mu\phi_0 + \frac{1}{2}\partial_\mu\phi_1\partial^\mu\phi_1 - V(\phi_0, \phi_1), \quad (3.1)$$

where  $R$  is Ricci scalar in Riemannian geometry. In order to obtain scale symmetry at the tree level one needs to assume a vanishing Higgs mass parameter  $m_H^2 = 0$ . In terms of

dilaton  $\phi_0$  and Higgs neutral component  $\phi_1$ , scale symmetric potential at the classical level is of the form:

$$V(\phi_0, \phi_1) = \lambda_0 \phi_0^4 + \lambda_1 \phi_0^2 \phi_1^2 + \lambda_2 \phi_1^4. \quad (3.2)$$

We choose certain hierarchy among couplings:

$$\lambda_2 \gg |\lambda_1| \gg \lambda_0 \quad (3.3)$$

and  $\lambda_2 > 0$ ,  $\lambda_1 < 0$ ,  $\lambda_0 > 0$ , so the new dilaton sector is weakly coupled to the Higgs sector.

Let us consider FLRW metric  $(1, -a(t)^2, -a(t)^2, -a(t)^2)$  with  $\sqrt{g} = \sqrt{|\det g|} = a(t)^3$ . Equations of motion from (3.1) for each field and  $g_{\mu\nu}$  are:

$$\begin{aligned} \phi_0 : \quad & \ddot{\phi}_0 + 3H\dot{\phi}_0 + \frac{\xi_0}{6}\phi_0 R + 4\lambda_0\phi_0^3 + 2\lambda_1\phi_0\phi_1^2 = 0 \\ \phi_1 : \quad & \ddot{\phi}_1 + 3H\dot{\phi}_1 + \frac{\xi_1}{6}\phi_1 R + 4\lambda_2\phi_1^3 + 2\lambda_1\phi_0^2\phi_1 = 0 \\ g_{\mu\nu} : \quad & \frac{1}{12}(\xi_0\phi_0^2 + \xi_1\phi_1^2)R - \frac{1}{2}\dot{\phi}_0^2 - \frac{1}{2}\dot{\phi}_1^2 + 2(\lambda_0\phi_0^4 + \lambda_1\phi_0^2\phi_1^2 + \lambda_2\phi_1^4) = 0 \end{aligned} \quad (3.4)$$

where  $H = \frac{\dot{a}}{a}$  is Hubble parameter. Stationary solutions give a flat direction:

$$\langle\phi_1^2\rangle = -\frac{\lambda_1}{2\lambda_2}\langle\phi_0^2\rangle, \quad \lambda_0 = \frac{\lambda_1^2}{4\lambda_2}, \quad \langle R \rangle = 0, \quad (3.5)$$

where the  $\lambda_0$  dependence comes from the condition of zero cosmological constant at the ground state:

$$V(\langle\phi_0\rangle, \langle\phi_1\rangle) = 0.$$

Since theory is scale symmetric, only ratios of mass scales can be determined and  $\langle\phi_0\rangle$  is arbitrary. With (3.3) we have the hierarchy  $\langle\phi_0\rangle \gg \langle\phi_1\rangle$ . When  $\phi_0$  acquires its vev, scale symmetry is broken and flat direction no longer exists. Because  $\langle\phi_1\rangle$  is proportional to  $\langle\phi_0\rangle$ , dilaton generates Higgs vev and mass, so it can be considered as origin of mass scales.

The mass matrix:

$$M^2 = \begin{pmatrix} \lambda_1 \left( 2\phi_1^2 + \frac{3\lambda_1}{\lambda_2}\phi_0^2 \right) & 4\lambda_1\phi_1\phi_0 \\ 4\lambda_1\phi_1\phi_0 & 2(6\lambda_2 + \lambda_1\phi_1^2\phi_0^2) \end{pmatrix}, \quad (3.6)$$

has two eigenvalues (at the ground state):

$$m_G^2 = 0, \quad m_H^2 = -4\lambda_1 \left( 1 - \frac{\lambda_1}{2\lambda_2} \right) \langle\phi_0^2\rangle, \quad (3.7)$$

so one of the eigenstates is massless (Goldstone associated with scale symmetry and flat direction).

### 3.1 Higgs potential parameters and Planck mass:

One can determine what values of  $\lambda_1$ ,  $\lambda_2$ ,  $\xi_0$  and  $\xi_1$  are available in our theory. First, we want hierarchy (3.3) and two conditions to be fulfilled:

$$m_H^2 = (125 \text{ GeV})^2, \quad \langle\phi_1\rangle = 250 \text{ GeV} \quad (3.8)$$

and in our model we have:

$$m_H^2 = -4\lambda_1 \left(1 - \frac{\lambda_1}{2\lambda_2}\right) \langle \phi_0^2 \rangle, \quad \langle \phi_1^2 \rangle = -\frac{\lambda_1}{2\lambda_2} \langle \phi_0^2 \rangle. \quad (3.9)$$

Satisfying all the conditions we get:

$$\lambda_2 = \frac{1}{32} \left(1 + 16\lambda_1\right), \quad -\frac{1}{48} \leq \lambda_1 \leq 0 \quad (3.10)$$

and example values are:

$$\lambda_2(\lambda_1 = -10^{-6}) \approx \lambda_2(\lambda_1 = -10^{-11}) \approx 0.03125. \quad (3.11)$$

Required value of  $\langle \phi_0 \rangle$  is then:

$$\langle \phi_0^2 \rangle = -\frac{2\lambda_2}{\lambda_1} \langle \phi_1^2 \rangle = -\frac{2\lambda_2}{\lambda_1} \cdot (250 \text{ GeV})^2. \quad (3.12)$$

Then, we want the Planck mass scale to be generated by  $\phi_i$  fields, as in (2.15):

$$\frac{1}{6} \left( \xi_0 - \frac{\lambda_1}{2\lambda_2} \xi_1 \right) \langle \phi_0^2 \rangle = M_{Planck}^2. \quad (3.13)$$

This will force constraints on values of  $\xi_i$  couplings. In realistic models, [7], we should have  $\xi_1 \ll \xi_0$ . Using (3.10), (3.12) and (3.13) we obtain relation of couplings:

$$\lambda_1 = \frac{-0.0625 \cdot \xi_0}{\xi_0 - \xi_1 + 1.43 \cdot 10^{34}}. \quad (3.14)$$

Example values:

$$\begin{aligned} \xi_0 = 10^5, \quad \xi_1 = 0.1 &\Rightarrow \lambda_1 = -4.37 \cdot 10^{-31}, \\ \xi_0 = 10^{10}, \quad \xi_1 = 0.1 &\Rightarrow \lambda_1 = -4.37 \cdot 10^{-26}, \\ \xi_0 = 10^{15}, \quad \xi_1 = 0.1 &\Rightarrow \lambda_1 = -4.37 \cdot 10^{-21}. \end{aligned} \quad (3.15)$$

## 4 Temperature corrections

### 4.1 Quantum Field Theory at finite temperature:

To obtain temperature corrections one adds to potential temperature dependent parts [19–21]:

$$V(\phi_0, \phi_1) \rightarrow V(\phi_0, \phi_1) + \delta V_T(\phi_0, \phi_1, T) + \delta V_{ring}(\phi_0, \phi_1, T). \quad (4.1)$$

$\delta V_T$  stands for standard temperature corrections of first order:

$$\delta V_T(\phi_0, \phi_1, T) = \frac{T^4}{2\pi^2} \left[ \sum_{i=\text{bosons}} n_i \cdot J_B\left(\frac{m_i^2(\phi_k)}{T^2}\right) + \sum_{j=\text{fermions}} n_j \cdot J_F\left(\frac{m_j^2(\phi_k)}{T^2}\right) \right], \quad (4.2)$$



where  $n_i$  and  $n_j$  are numbers of degrees of freedom of considered boson or fermion particle with field-dependent mass  $m_i(\phi_k)$  and  $J_B$  and  $J_F$  are thermal bosonic (B) or fermionic (F) functions defined as follows:

$$J_B\left(\frac{m^2}{T^2}\right) = \int_0^\infty dx \cdot x^2 \log\left(1 - e^{-\sqrt{x^2 + \frac{m^2}{T^2}}}\right), \quad (4.3)$$

$$J_F\left(\frac{m^2}{T^2}\right) = \int_0^\infty dx \cdot x^2 \log\left(1 + e^{-\sqrt{x^2 + \frac{m^2}{T^2}}}\right). \quad (4.4)$$

One should also add infrared contributions from higher order diagrams [19], which are of the same order as corrections from (4.2):

$$\delta V_{ring} = -\frac{T}{12\pi} \left( m_{eff}(\phi_i, T)^3 - m_i(\phi_i)^3 \right), \quad (4.5)$$

which is the so-called ring improvement of the potential and is sufficient for high temperatures, when  $(m/T) \ll 1$ . Temperature-dependent masses  $m_{eff}(\phi_i, T)$ , can be obtained from high temperature expansion of:

$$V + \delta V_T \Big|_{m/T \ll 1}. \quad (4.6)$$

### Particle content and thermal masses

Obviously, the degrees of freedom  $\phi_0$  and  $\phi_1$  are present in our theory, and the mass eigenstates are their mixture. So we have two neutral scalars  $G$  (massless Goldstone) and  $H$  (massive "Higgs") with  $n_G = n_H = 1$ . The masses of this sector are the eigenvalues of (3.6):

$$\begin{aligned} m_G^2 &= 2\lambda_1 \phi_1^2 + \mathcal{O}(\lambda_1^2) \\ m_H^2 &= 12\lambda_2 \phi_1^2 + 2\lambda_1 \phi_0^2 + \mathcal{O}(\lambda_1^2). \end{aligned} \quad (4.7)$$

However, there are particles in SM, which give important contributions to (4.2). These are:

- $W^\pm$  boson:  $m_W^2 = \frac{1}{4}g_2^2\phi_1^2$ ,  $n_w = 6$ ,
- $Z$  boson:  $m_Z^2 = \frac{1}{4}(g_1^2 + g_2^2)\phi_1^2$ ,  $n_Z = 3$
- top quark:  $m_t^2 = \frac{1}{2}h_t^2\phi_1^2$ ,  $n_t = -12$ ,

where  $g_1 \approx 0.35$ ,  $g_2 \approx 0.65$  and  $h_t \approx 1$  are correspondingly weak, strong and top yukawa coupling constants.

From (4.6) we obtain the mass matrix:

$$\begin{aligned} \begin{pmatrix} m_{00} & m_{10} \\ m_{01} & m_{11} \end{pmatrix}_{eff} &= \begin{pmatrix} \frac{\partial^2 V}{\partial \phi_0^2} & \frac{\partial^2 V}{\partial \phi_1 \partial \phi_0} \\ \frac{\partial^2 V}{\partial \phi_0 \partial \phi_1} & \frac{\partial^2 V}{\partial \phi_1^2} \end{pmatrix} + \\ &+ \begin{pmatrix} \left(\frac{\lambda_1}{6} + \frac{\lambda_1^2}{4\lambda_2}\right)T^2 & 0 \\ 0 & \left(\lambda_2 + \frac{\lambda_1}{6} + \frac{g_1^2}{16} + \frac{3g_2^2}{16} + \frac{h_t^2}{4}\right)T^2 \end{pmatrix}. \end{aligned} \quad (4.8)$$

The thermal masses  $m_{eff}^2$  for scalars are the eigenvalues of this matrix:

$$\begin{aligned}(m_G^2)_{eff} &= 2\lambda_1\phi_1^2 + \frac{\lambda_1}{6}T^2 + \mathcal{O}(\lambda_1^2), \\ (m_H^2)_{eff} &= 12\lambda_2\phi_1^2 + 2\lambda_1\phi_0^2 + \left(\lambda_2 + \frac{\lambda_1}{6} + \frac{g_1^2}{16} + \frac{3g_2^2}{16} + \frac{h_t^2}{4}\right)T^2 + \mathcal{O}(\lambda_1^2).\end{aligned}\tag{4.9}$$

It should be noted, that the dependence of the temperature corrections on  $\phi_0$  enters via the tree-level mass terms in the scalar sector. Moreover, since the hierarchy of scales demands the hierarchy of couplings, one finds in the present case  $\lambda_0 = \frac{\lambda_1^2}{4\lambda_2} \ll |\lambda_1| \ll \lambda_2$  and the dependence on  $\phi_0$  starts at the linear order in a small coupling  $\lambda_1$ . At this point we refrain from discussing the issue of thermal equilibrium of the whole system and concentrate on the analysis of the thermal effective potential.

## 4.2 Symmetry breaking at high temperature

The scale symmetry breaking can be discussed reliably at the leading level of high temperature expansion, where

$$V_{eff} = V_{T=0} + \frac{1}{2}\phi_1^2 \cdot \left(\lambda_2 + \frac{\lambda_1}{6} + \frac{g_1^2}{16} + \frac{3g_2^2}{16} + \frac{h_t^2}{4}\right)T^2 + \frac{1}{2}\phi_0^2 \cdot \frac{\lambda_1}{6}T^2 = V_{T=0} + \frac{\gamma T^2}{2}\phi_1^2 + \frac{\lambda_1 T^2}{12}\phi_0^2.\tag{4.10}$$

One should note that the coefficients of the two terms quadratic in the temperature are completely independent, as in the case of  $\phi_1$ , which plays the role of the Higgs field, the thermal corrections are dominated by gauge couplings and by the coupling to the top quark, whereas in the case of the  $\phi_0$  they are proportional to the coupling of the mixing term in the scalar sector. As the result, the proportionality of the two scalar equations of motion which holds at  $T = 0$  gets broken by the term

$$\left(\frac{\lambda_1}{6} - \gamma\right)T^2 \neq 0.\tag{4.11}$$

This is the amount of the scale symmetry breaking by the finite temperature effects. As the result, the only consistent solution to the corrected equations of motion becomes at this order

$$\phi_1 = 0, \quad \phi_0 = -\frac{\lambda_2}{6\lambda_1}T^2.\tag{4.12}$$

This shows, that at finite temperature the minimum of the potential picks up a finite expectation value of the dilaton underlying the fact that the scale symmetry remains broken, and the scale of the breaking given by the vev of the dilaton is proportional to the temperature - the new scale in the system. However, this indicates, that when the temperature goes to zero, the symmetry gets restored and the system goes into the unbroken phase, since the vevs of both scalars seem to be led to the origin. One should note that this would restore also the electroweak symmetry, which requires a nonvanishing vev of  $\phi_0$ . The point is that it is this vev which multiplied by the negative coupling  $\lambda_1$  plays the role of the negative mass squared term in the Higgs sector. This would suggest a symmetric, unrealistic, vacuum emerging from the hot phase of the universe. However, the situation is more subtle. The point is that the Higgs field  $\phi_1$  easily comes to the equilibrium with rest of the universe

through interaction with the Standard Model matter and gauge fields, which despite the fact that its thermal average seems to vanish, produces a large rms value of the order of

$$\langle \phi_1^2 \rangle_{T,p} = T \frac{p^3}{\omega_p^2} \quad (4.13)$$

per decade. For high temperatures and small masses this can be approximated as  $T^2$ , and produces a large repulsive force in the equation of motion of  $\phi_0$  due to the mixing term in the potential

$$\delta_m V = \lambda_1 \phi_0^2 \phi_1^2 \rightarrow \lambda_1 T^2 \phi_0^2, \quad (4.14)$$

giving in the eom the contribution

$$-\frac{\partial \delta_m V}{\partial \phi_0} = -2\lambda_1 T^2 \phi_0, \quad (4.15)$$

which drives the dilaton away from the origin. In addition, as discussed later, the dynamical thermal equilibrium in the scalar sector, perhaps after the point of quasi-thermal initial production, is not to be maintained at the later stages of the evolution of the universe. Hence, in the realistic physical system the origin will not be achieved globally and there will be in the universe domains characterized by large expectation value of the dilaton, and hence the Higgs, which when the temperature drops down will have a chance to evolve dynamically into the zero temperature vacuum with spontaneously broken scale symmetry and electroweak symmetry. The possible late time dynamics of such systems shall be discussed in the Section 5.

#### 4.2.1 Numerical analysis

Here we show numerical results of how thermal corrections change the potential. The results nicely illustrate the approximate analytic picture presented in the previous section. To make plots more clear we choose the value of the coupling to be  $\lambda_1 = -10^{-6}$ .

As one expects, temperature corrections break the scale symmetry. In Figure (1) one can see that for higher temperatures, the flat direction no longer exists (Figure 2) and there is visible a local minimum. We made it better visible in Figures 3 and 4, where  $\phi_i$  directions are plotted. Temperature corrections drive  $\phi_1$  to zero value. The dilaton field minimum then becomes:

$$\begin{aligned} \phi_0^2 = & \left[ \frac{(9.89\alpha - 3.63\lambda_2 - 6.91 \cdot 10^{-16}g_1^2 - 2.76 \cdot 10^{-15}h_t^2)}{(-39.48\alpha + \lambda_2(\alpha \log(-\lambda_1) + 3.48\alpha + 43.53))} + \right. \\ & \left. + \frac{\lambda_2(6.58\alpha - 43.53\lambda_2 - 2.72g_1^2 - 8.16g_2^2 - 10.88h_t^2)}{\lambda_1(-39.48\alpha + \lambda_2(\alpha \log(-\lambda_1) + 3.48\alpha + 43.53))} \right] \cdot T^2, \end{aligned} \quad (4.16)$$

where

$$\alpha = \sqrt{48\lambda_2 + 3g_1^2 + 9g_2^2 + 12h_t^2}. \quad (4.17)$$

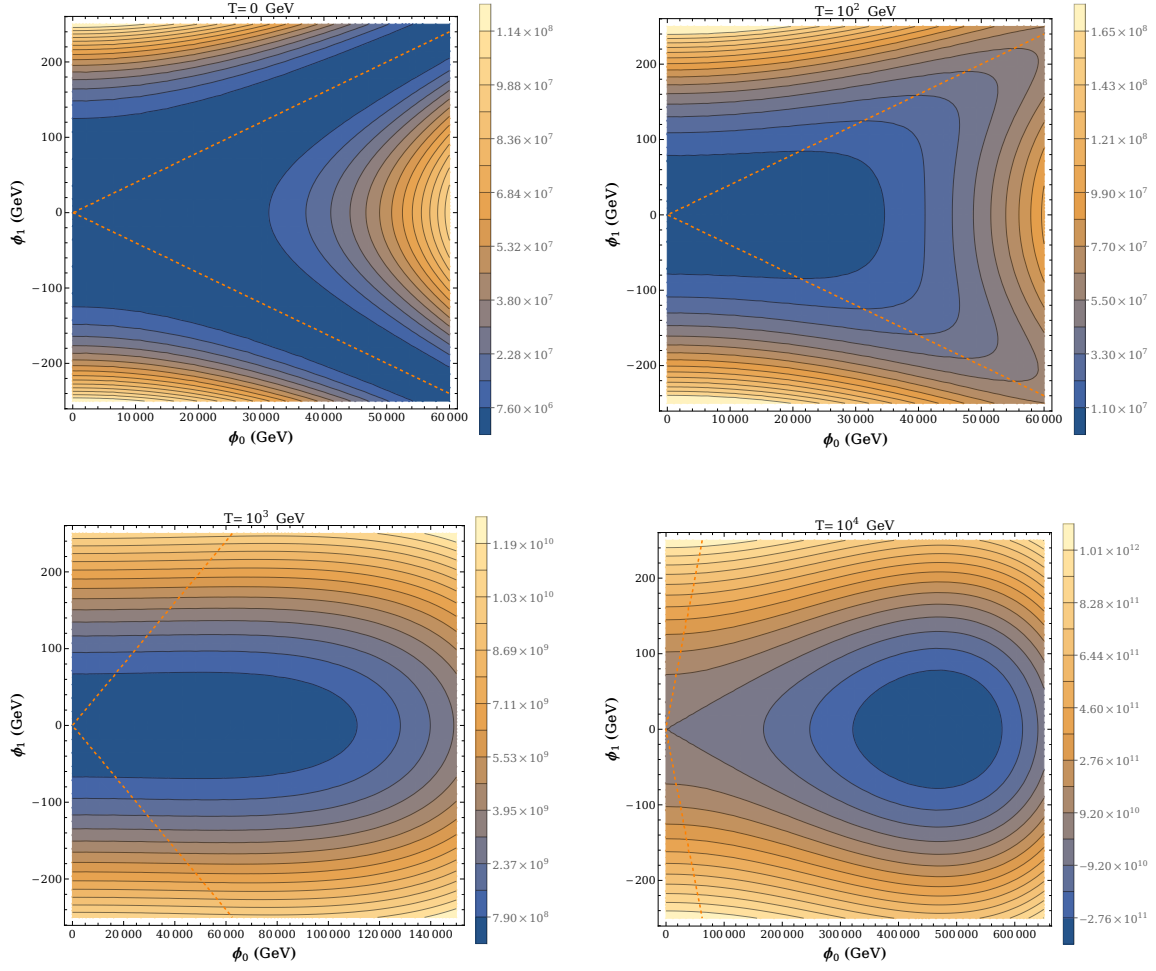


**Figure 1:** Plots of  $V_{full}(\phi_0, \phi_1, T)$  for different temperatures and  $\lambda_1 = -10^{-6}$ . Orange dashed line marks flat direction  $\phi_1^2 = -\frac{\lambda_1}{2\lambda_2}$ . It is easy to see that as the temperature increase, the flat direction no longer exists and the scale symmetry is broken.

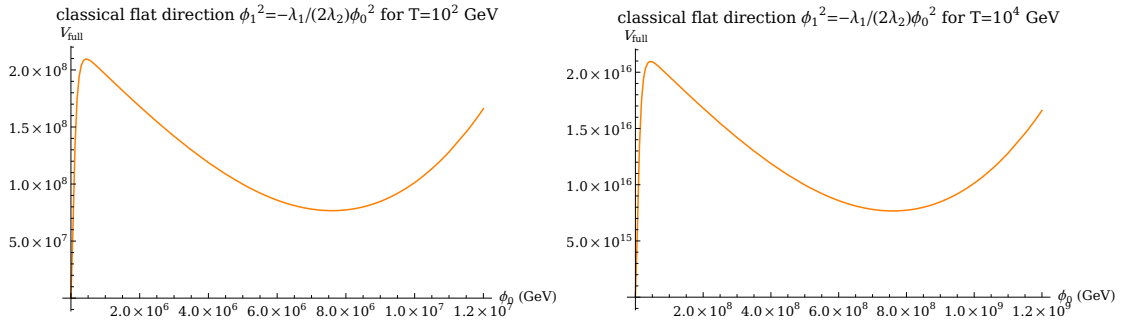


**Figure 2:** Classical flat direction is spoiled for non-zero temperatures.

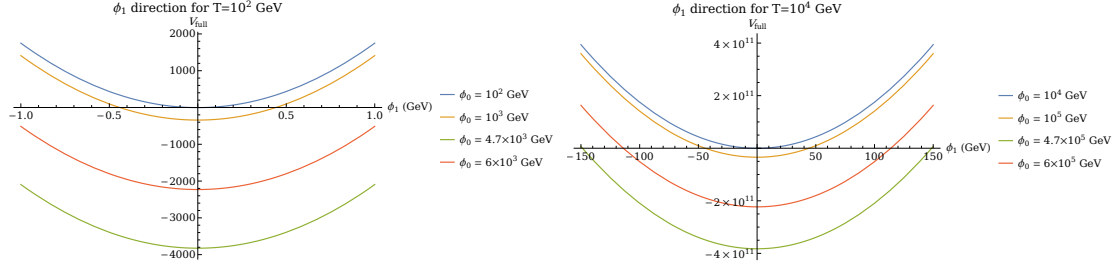


**Figure 3:**  $\phi_1$  direction of  $V_{full}(\phi_0, \phi_1, T)$  for 2 different temperatures and various  $\phi_0$  values. The lowest curve corresponds to  $\phi_0$  from high temperature minimum (4.16).

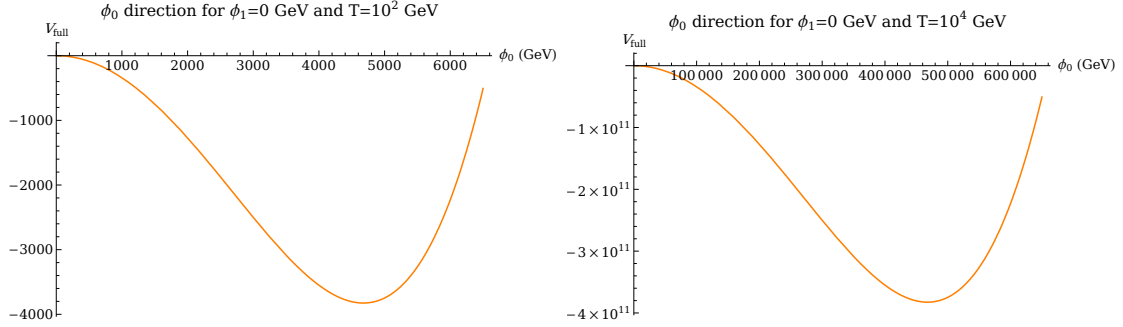


**Figure 4:**  $\phi_0$  direction of  $V_{full}(\phi_0, \phi_1, T)$  for 2 different temperatures and  $\phi_1 = 0$ . There's visible minimum at  $\phi_0 \approx 4.7 \cdot 10 \cdot T$ , which corresponds to equation (4.16).

### 4.3 Thermal equilibrium

To discuss physical applications of the scale symmetric models, one needs to consider the issue of thermal equilibrium.

First, let us investigate in which temperature range the  $\phi_0$  is in thermal equilibrium. To do so, one needs to calculate a cross section [16]:

$$\frac{d\sigma}{dt} = \frac{1}{64\pi \cdot s} \frac{1}{|\vec{p}_{1CM}|^2} |\mathcal{M}|^2, \quad (4.18)$$

where  $s$  and  $t$  are Mandelstam variables and  $\vec{p}_{1CM}$  is momentum of an in-going particle in the center of mass frame. All essential steps and formulae are to be found in [16]. We also use following approximations:

$$m_{\phi_0} \approx m_G = 0, \quad m_{\phi_1} \approx m_H = 125 \text{ GeV}. \quad (4.19)$$

The only  $\phi_0\phi_1$  interaction present in  $V$  is  $\lambda_1\phi_0^2\phi_1$  with  $|\mathcal{M}|^2 = 16\lambda_1^2$ . So there are two processes:

- INELASTIC  $\phi_0\phi_1 \rightarrow \phi_0\phi_1$ :

$$\sigma(s) = \frac{\lambda_1^2}{\pi \cdot s},$$

- ELASTIC  $\phi_1\phi_1 \rightarrow \phi_0\phi_0$ :

$$\sigma(s) = \frac{\lambda_1^2}{\pi \sqrt{s(s - 4m_H^2)}}.$$

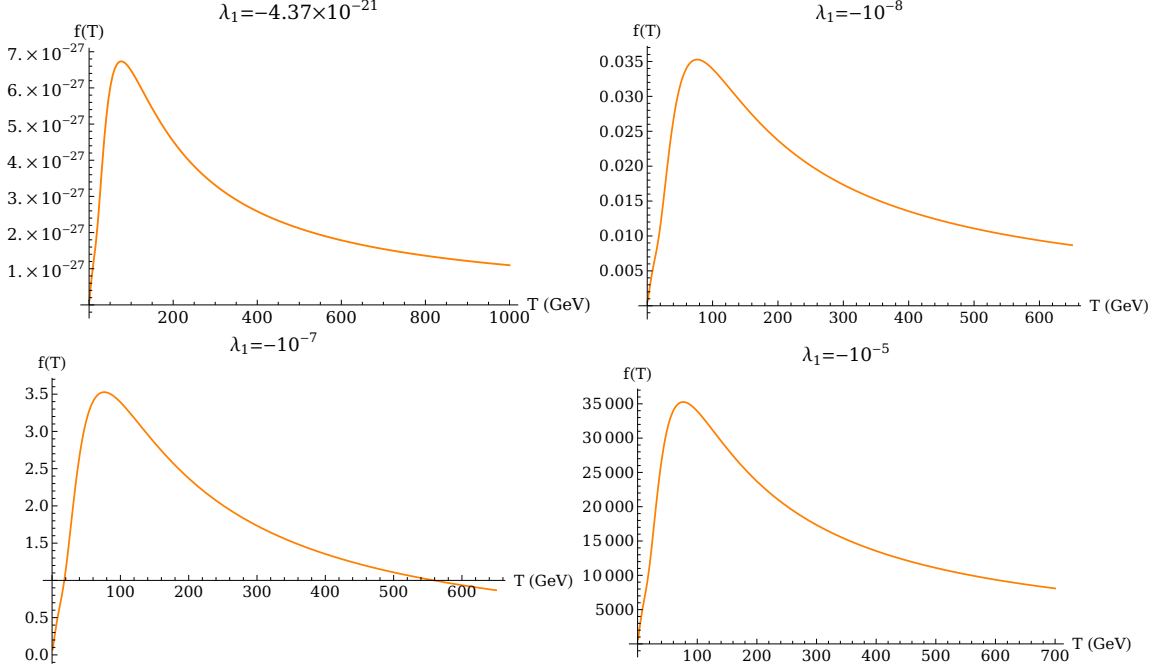


**Figure 5:** Ratio  $f(T) = (T^3\langle\sigma v\rangle)/H$  as a function of temperature for different  $\lambda_1$ .  $\phi_0$  field can reach thermal equilibrium for sufficiently large  $|\lambda_1|$  value.

Next, thermally averaged cross section for elastic process  $\phi_0\phi_1 \rightarrow \phi_0\phi_1$  is of the form [17]:

$$\langle\sigma \cdot v\rangle_{EL} = \frac{1}{16K_2(m_H/T) \cdot m_H^2 T^3} \int_{m_H^2}^{\infty} ds \cdot \lambda(s, m_H, 0) \frac{\sigma(s)}{\sqrt{s}} K_1(\sqrt{s}/T) \quad (4.20)$$

and for inelastic process  $\phi_1\phi_1 \rightarrow \phi_0\phi_0$  [17]:

$$\langle\sigma \cdot v\rangle_{INEL} = \frac{1}{8K_2(m_H/T)^2 \cdot m_H^4 T} \int_{m_H^2}^{\infty} ds \cdot \lambda(s, m_H, m_H) \frac{\sigma(s)}{\sqrt{s}} K_1(\sqrt{s}/T), \quad (4.21)$$

where  $K_i(x)$  is a modified Bessel function of  $i$ -th kind and

$$\lambda(x, y, z) = [x - (y + z)^2] \cdot [x - (y - z)^2].$$

Particles are in thermal equilibrium as long as their interaction rate  $\Gamma$  satisfies:

$$\Gamma \gtrsim H, \quad (4.22)$$

where  $H$  is Hubble parameter, and for radiation dominated era it is of the form

$$H(T) = \frac{1}{\sqrt{3}m_{Pl}} \sqrt{\frac{\pi^2}{30} g_* T^4}, \quad (4.23)$$

where  $g_*$  is the number of effective degrees of freedom of relativistic particles in hot Universe and Planck mass is  $m_{Pl} = 2.4354 \cdot 10^{18}$  GeV. Interaction rate is proportional to the thermally

averaged cross section  $\Gamma \sim T^3 \langle \sigma v \rangle$ , hence we can examine ratio  $(T^3 \langle \sigma v \rangle)/H = f(T)$  as a function of temperature, where

$$\langle \sigma v \rangle = \langle \sigma v \rangle_{EL} + \langle \sigma v \rangle_{INEL}. \quad (4.24)$$

For temperatures above 0.1 GeV we have  $g_* \approx 100$  [22]. We show the results for different  $\lambda_1$  on Figure 5. Dilaton  $\phi_0$  can reach the equilibrium state for  $\lambda_1 \gtrsim -10^{-7}$ .

## 5 Time evolution of the fields

In this section, we shall investigate numerically the evolution of the scale symmetric scalar sector in the expanding universe. We show that there exist reasonable initial conditions which lead to the physically relevant vacuum configuration at the very late stages of the evolution.

### 5.1 Zero temperature

We use equations of motion (3.4) with relation  $R = 12H^2 + 6\dot{H}$ :

$$\begin{aligned} \ddot{\phi}_0 + 3H\dot{\phi}_0 + 2\xi_0\phi_0^2H^2 + \xi_0\phi_0^2\dot{H} + 4\lambda_0\phi_0^3 + 2\lambda_1\phi_0\phi_1^2 &= 0 \\ \ddot{\phi}_1 + 3H\dot{\phi}_1 + 2\xi_1\phi_1^2H^2 + \xi_1\phi_1^2\dot{H} + 4\lambda_2\phi_1^3 + 2\lambda_1\phi_0^2\phi_1 &= 0 \\ \frac{1}{2}(\xi_0\phi_0^2 + \xi_1\phi_1^2)(2H + \dot{H}) - \frac{1}{2}\dot{\phi}_0^2 - \frac{1}{2}\dot{\phi}_1^2 + 2(\lambda_0\phi_0^4 + \lambda_1\phi_0^2\phi_1^2 + \lambda_2\phi_1^4) &= 0 \end{aligned} \quad (5.1)$$

We treat the Hubble parameter as an independent variable, which dynamics is ruled by above equations. Fixed points of (5.1) are:

$$\langle \phi_1^2 \rangle = -\frac{\lambda_1}{2\lambda_2} \langle \phi_0^2 \rangle, \quad \langle H \rangle = 0. \quad (5.2)$$

### Example evolution solutions

All initial conditions used in simulations are provided under plots in the figure captions. Two initial Hubble parameter  $H(0) = H_0$  values were chosen: 0.1 and 0.5. Since  $H$  is a magnitude of expansion, hence it can be interpreted as a parameter describing how fast  $\phi_i$  fields loose their energy. Bigger  $H_0$  values result in faster velocity  $\phi'_i$  damping and lower final values  $\langle \phi_i \rangle$ . We choose two parameter spaces: one with realistic  $\lambda_i$  and  $\xi_i$  values, fulfilling requirements from section 3.1 and one with bigger  $|\lambda_1|$  and smaller  $\xi_0$ . In both cases  $\phi_i$  fields stop to evolve after sufficiently long time and settle at some point of the flat direction  $\langle \phi_1^2 \rangle = -\frac{\lambda_1}{2\lambda_2} \langle \phi_0^2 \rangle$ . Of course, the arrow of the initial velocity might play a role, but this is a direct choice and we always pick up the velocity direction, which enhances the effects.

- realistic model:  $\lambda_2 = 0.03125$ ,  $\lambda_1 = -4.37 \cdot 10^{-26}$ ,  $\xi_0 = 10^{10}$ ,  $\xi_1 = 0.1$

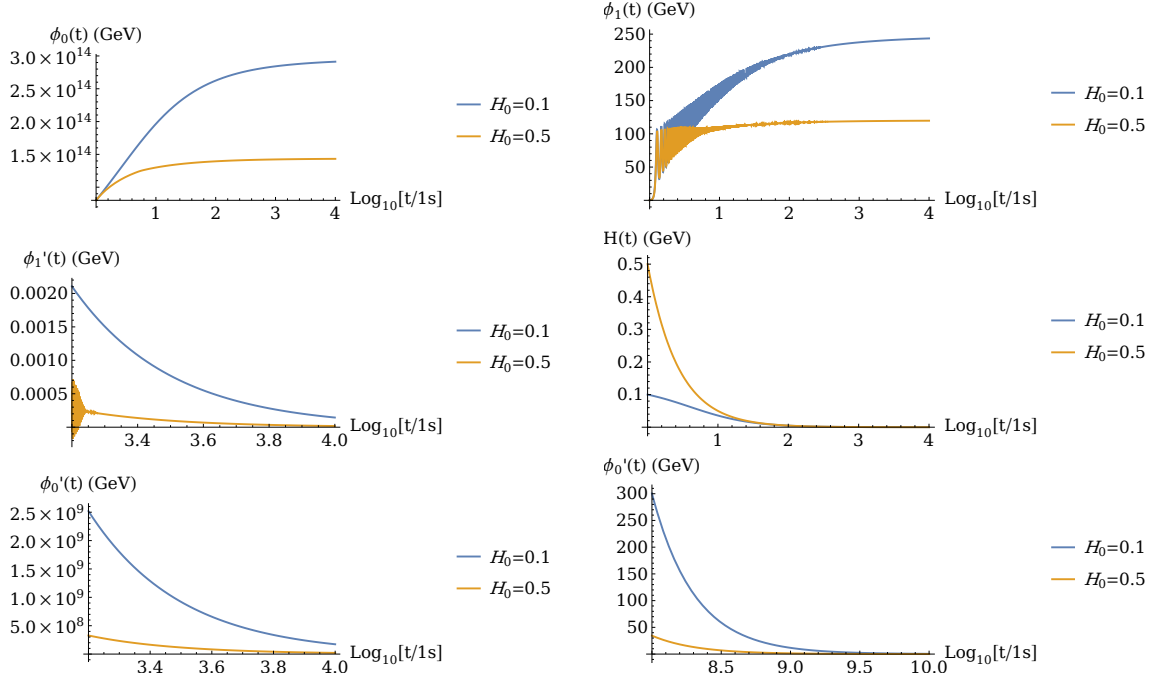


**Figure 6:** Evolution of  $\phi_i$  fields and  $H$  with time for coupling constants values fulfilling requirements from section 3.1:  $\lambda_2 = 0.03125$ ,  $\lambda_1 = -4.37 \cdot 10^{-26}$ ,  $\xi_0 = 10^{10}$ ,  $\xi_1 = 0.1$ . Initial conditions:  $\phi_0(0) = 8 \cdot 10^{13}$ ,  $\dot{\phi}_0(0) = 5 \cdot 10^{13}$ ,  $\phi_1(0) = 0$ ,  $\dot{\phi}_1(0) = 10$ , and two different  $H(0) = H_0$  values. The bigger the initial  $H_0$ , the faster  $\phi_i$  fields loose their velocity and settles in lower values. Two plots for  $\phi_0'(t)$  are shown, one for the same time range as in the evolution of  $\phi_1$  and  $H$ , one for later times, to show that  $\phi_0$  indeed loose its velocity and settles in desired value.

- unrealistic model:  $\lambda_2 = 0.03125$ ,  $\lambda_1 = -10^{-6}$ ,  $\xi_0 = 10^3$ ,  $\xi_1 = 0.1$

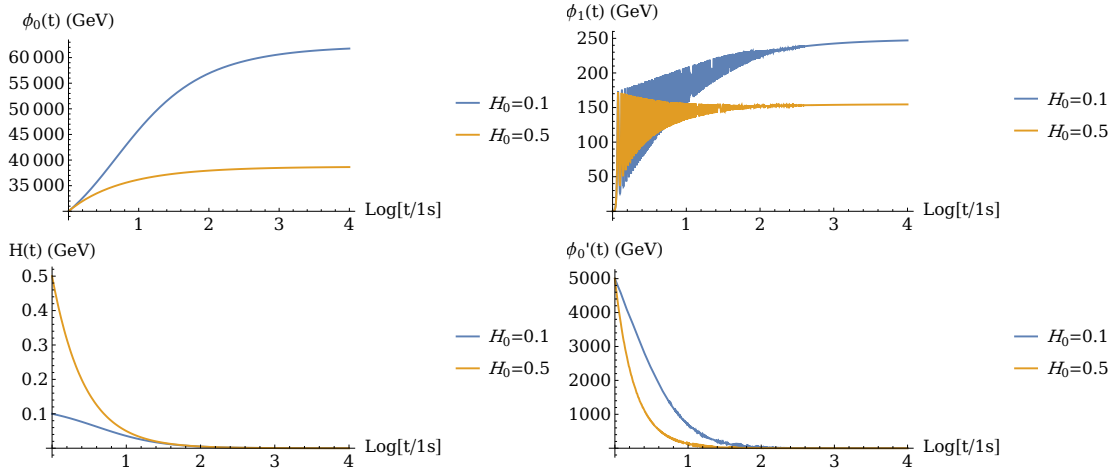


**Figure 7:** Evolution of  $\phi_i$  fields and  $H$  with time for coupling constants values:  $\lambda_2 = 0.03125$ ,  $\lambda_1 = -10^{-6}$ ,  $\xi_0 = 10^3$ ,  $\xi_1 = 0.1$ . Initial conditions:  $\phi_0(0) = 3 \cdot 10^4$ ,  $\dot{\phi}_0(0) = 5 \cdot 10^3$ ,  $\phi_1(0) = 0$ ,  $\dot{\phi}_1(0) = 10$  and two different  $H(0) = H_0$  values. The bigger the initial  $H_0$ , the faster  $\phi_i$  fields loose their velocity and settles in lower values.



## 5.2 Non-zero temperature

To examine evolution of fields  $\phi_0$  and  $\phi_1$  with time in a hot universe, we use equations of motion (3.4) corrected by thermal masses. Hence, we add to the potential  $V$  the terms:

$$V_{eff} = V + \frac{1}{2}\phi_1^2 \cdot \left( \lambda_2 + \frac{\lambda_1}{6} + \frac{g_1^2}{16} + \frac{3g_2^2}{16} + \frac{h_t^2}{4} \right) T^2 + \frac{1}{2}\phi_0^2 \cdot \frac{\lambda_1}{6} T^2. \quad (5.3)$$

We assume a temperature dependence ruled by radiation:

$$T(t) = \frac{1.121 \cdot \text{GeV} \cdot \sqrt{s}}{\sqrt{t + t_0}}, \quad (5.4)$$

where  $t_0$  is chosen to fit the initial eligible temperature of evolution  $T_0$ . During this epoch, the contribution of radiation to the Hubble parameter is less than about  $10^{-10}$  GeV for temperatures below  $10^4$  GeV. Therefore, we neglect this contribution and treat  $H$  as an independent parameter ruled by the equations of motion (3.4).

In general, the mechanism of kinetic energy dissipation via cosmic friction is sensitive to the chosen coupling value  $\lambda_1$  and to the initial value of the Hubble parameter. If the chosen value of  $\lambda_1$  is too large in magnitude, the temperature-dependent contribution to the equation of motion gives the dilaton a large velocity so that the damping due to expansion is not sufficient and at low temperature the dilaton lands in the flat direction of the potential with a large velocity and moves away towards large field values, i.e. large mass scales. Example evolution with  $\lambda_1 = -10^{-2}$  is shown on Figure 10.

### Example evolution solutions

To show differences in evolution with temperature, we choose the same initial conditions and parameter space values as in  $T = 0$  case. For  $\lambda_1 = -4.37 \cdot 10^{-26}$ ,  $\phi_0$  field is not in thermal equilibrium, hence  $\phi_0^2 T^2$  term from (5.3) is absent in equations of motion.

- realistic model, dilaton never in thermal equilibrium:  $\lambda_2 = 0.03125$ ,  $\lambda_1 = -4.37 \cdot 10^{-26}$ ,  $\xi_0 = 10^{10}$ ,  $\xi_1 = 0.1$

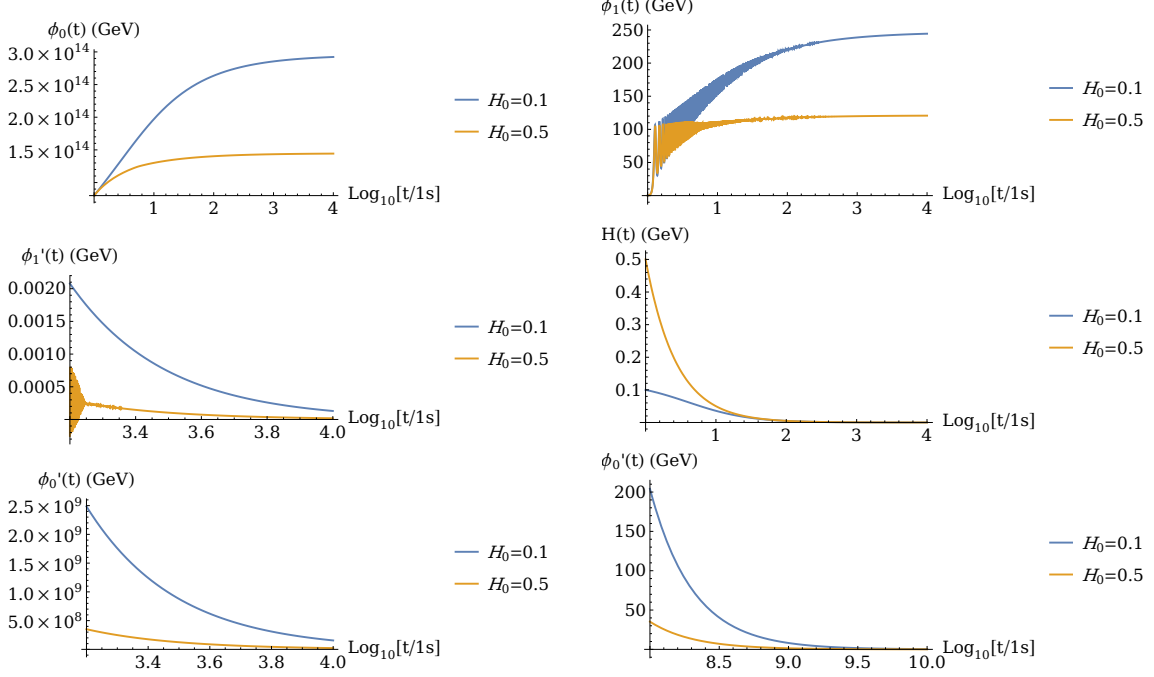


**Figure 8:** Evolution of  $\phi_i$  fields and  $H$  with time for non-zero temperature and coupling constants values fulfilling requirements from section 3.1:  $\lambda_2 = 0.03125$ ,  $\lambda_1 = -4.37 \cdot 10^{-26}$ ,  $\xi_0 = 10^{10}$ ,  $\xi_1 = 0.1$ . Initial conditions:  $\phi_0(0) = 8 \cdot 10^{13}$ ,  $\dot{\phi}_0(0) = 5 \cdot 10^{13}$ ,  $\phi_1(0) = 0$ ,  $\dot{\phi}_1(0) = 10$  and two different  $H(0) = H_0$  values. Initial temperature  $T_0 = 10^4$  GeV.

- unrealistic model, dilaton in thermal equilibrium:  $\lambda_2 = 0.03125$ ,  $\lambda_1 = -10^{-6}$ ,  $\xi_0 = 10^3$ ,  $\xi_1 = 0.1$

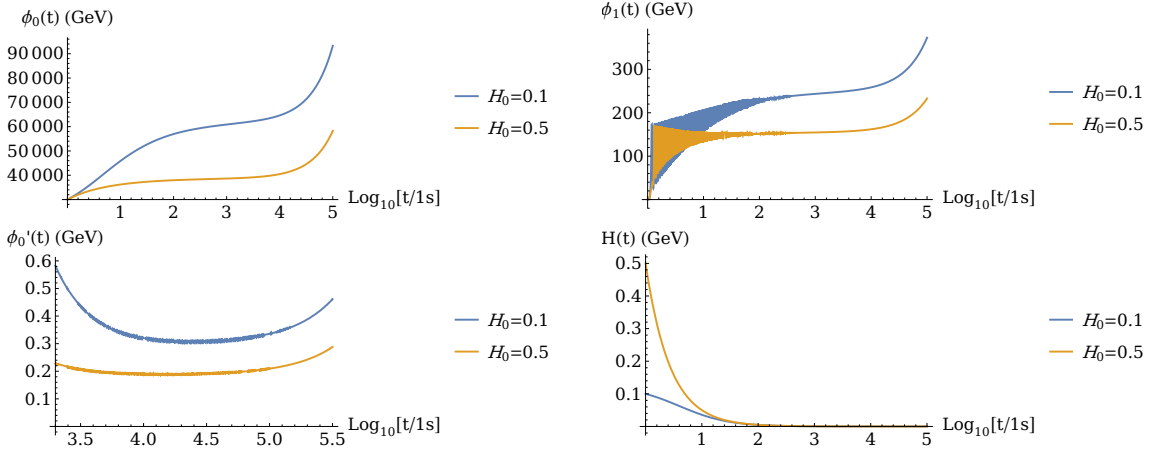


**Figure 9:** Evolution of  $\phi_i$  fields and  $H$  with time for non-zero temperature and coupling constants values  $\lambda_2 = 0.03125$ ,  $\lambda_1 = -10^{-6}$ ,  $\xi_0 = 10^3$ ,  $\xi_1 = 0.1$ . Initial conditions:  $\phi_0(0) = 3 \cdot 10^4$ ,  $\dot{\phi}_0(0) = 5 \cdot 10^3$ ,  $\phi_1(0) = 0$ ,  $\dot{\phi}_1(0) = 10$  and two different  $H(0) = H_0$  values. Initial temperature  $T_0 = 10^4$  GeV. After fields  $\phi_i$  land in flat direction, they start to roll along that flat valley to higher values and they don't stop.

- unrealistic model, dilaton in thermal equilibrium:  $\lambda_2 = 0.02625$ ,  $\lambda_1 = -10^{-2}$ ,  $\xi_0 = 10^3$ ,  $\xi_1 = 0.1$

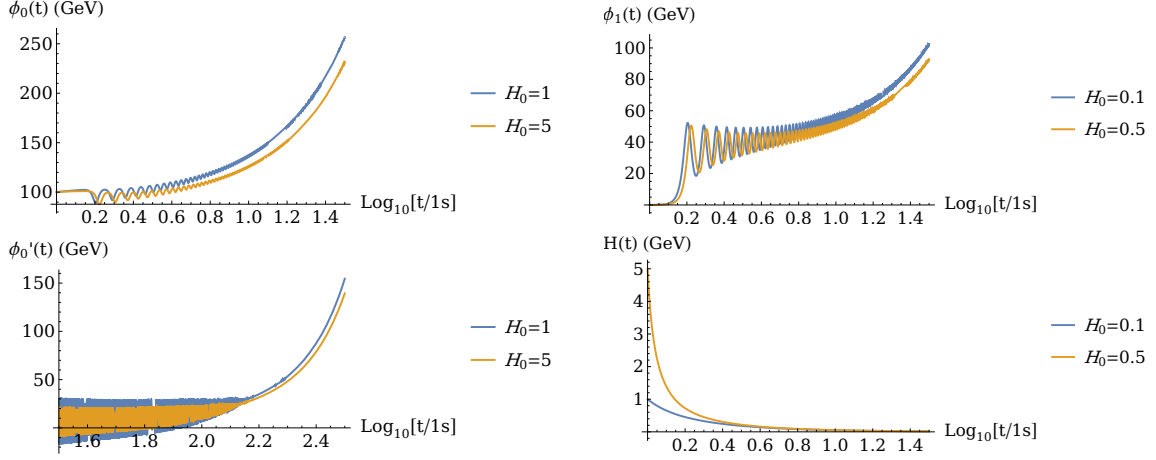


**Figure 10:** Evolution of  $\phi_i$  fields and  $H$  with time for non-zero temperature and coupling constants values  $\lambda_2 = 0.02625$ ,  $\lambda_1 = -10^{-2}$ ,  $\xi_0 = 10^3$ ,  $\xi_1 = 0.1$ . Initial conditions:  $\phi_0(0) = 100$ ,  $\dot{\phi}_0(0) = 10$ ,  $\phi_1(0) = 0$ ,  $\dot{\phi}_1(0) = 1$ , and two different  $H(0) = H_0$  values. Initial temperature  $T_0 = 10^4$  GeV. After fields  $\phi_i$  land in flat direction, they start to roll along that flat valley to higher values.

### 5.3 $T = 0$ vs $T \neq 0$

In Figure 11 we provided comparison of evolution for zero and non-zero temperature with  $H_0 = 0.1$  and physical values of coupling constants. Adding temperature changes the speed of field velocity loss. In hot Universe the most dominant thermal contribution to the force controlling evolution of  $\phi'_i$  comes from  $\phi_1^2 T^2$  term:

$$-\frac{\partial V}{\partial \phi_1} \sim -\phi_1 \left( \lambda_2 + \frac{\lambda_1}{6} + \frac{g_1^2}{16} + \frac{3g_2^2}{16} + \frac{h_t^2}{4} \right) T^2 < 0 \quad (5.5)$$

and it is negative. Hence, for non-zero temperatures, fields are stopped more efficiently, but it doesn't affect the final point of their evolution.

The case is different though if we choose bigger absolute value of  $\lambda_1$ , e.g.  $|\lambda_1| = 10^{-6}$  as it is shown Figure 12. First, evolution is the same but at later times, both fields move further along flat direction. This happens because if the chosen value of  $\lambda_1$  is too large in magnitude, the temperature-dependent contribution to the equation of motion gives the dilaton some velocity so when it lands in the flat direction, the damping due to expansion is not sufficient and fields start to move away towards large field values i.e. large mass scale.

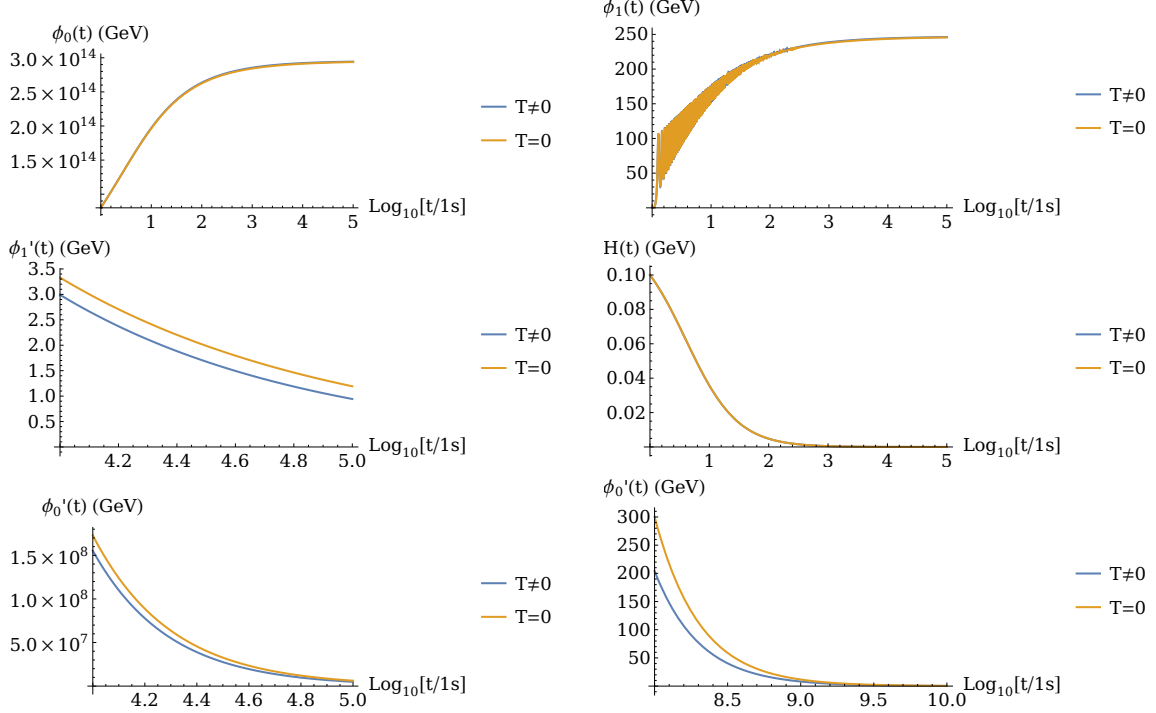


**Figure 11:** Evolution of  $\phi_i$  fields and  $H$  with time for zero and non-zero temperatures and with coupling constants' values fulfilling requirements from section 3.1:  $\lambda_2 = 0.03125$ ,  $\lambda_1 = -4.37 \cdot 10^{-26}$ ,  $\xi_0 = 10^{10}$ ,  $\xi_1 = 0.1$ . Initial conditions:  $\phi_0(0) = 8 \cdot 10^{13}$ ,  $\dot{\phi}_0(0) = 5 \cdot 10^{13}$ ,  $\phi_1(0) = 0$ ,  $\dot{\phi}_1(0) = 10$  and two different  $H(0) = H_0$  values. Initial temperature  $T_0 = 10^4$  GeV. The differences are very subtle. For  $T \neq 0$  kinetic energy drops down faster, but final values  $\langle \phi_i \rangle$  are practically the same for both evolutions.

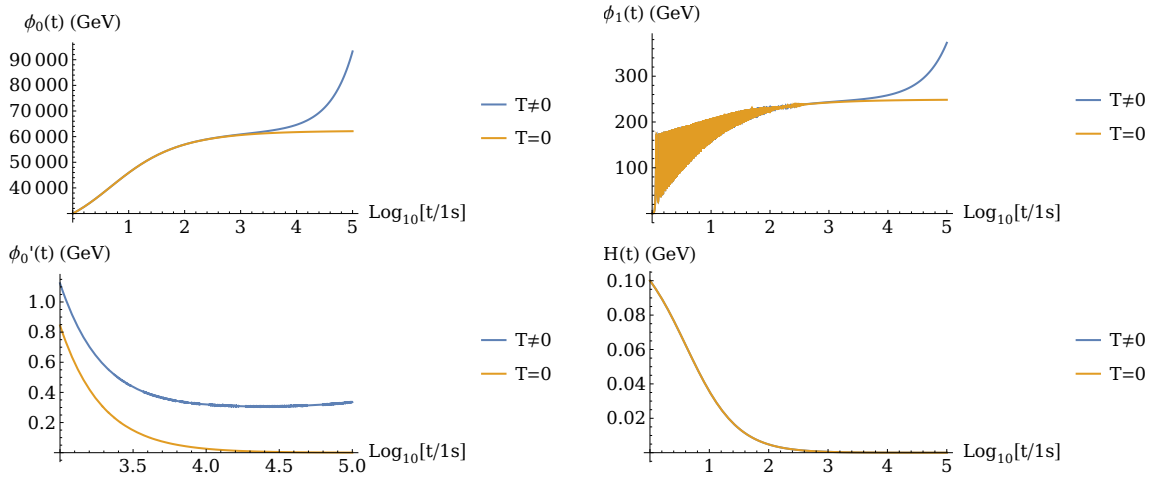


**Figure 12:** Evolution of  $\phi_i$  fields and  $H$  with time for zero and non-zero temperature and coupling constants values:  $\lambda_2 = 0.03125$ ,  $\lambda_1 = -10^{-6}$ ,  $\xi_0 = 10^3$ ,  $\xi_1 = 0.1$ . Initial conditions:  $\phi_0(0) = 3 \cdot 10^4$ ,  $\dot{\phi}_0(0) = 5 \cdot 10^3$ ,  $\phi_1(0) = 0$ ,  $\dot{\phi}_1(0) = 10$ , and two different  $H(0) = H_0$  values. Initial temperature  $T_0 = 10^4$  GeV. Because  $\lambda_1$  is not small enough, in non-zero temperature  $\phi_i$  fields don't settle at any final value, but start to roll down along flat direction.

## 5.4 Electroweak Symmetry Breaking

To examine EWSB in our model, we consider time evolution of the effective potential  $V_{eff}$  (5.3) for the Higgs neutral component  $\phi_1$ , i.e.:

$$V_{\phi_1}(t) \equiv V_{eff}(\phi_0(t), \phi_1, T(t)), \quad (5.6)$$

where  $\phi_0(t)$  comes from solution of evolution for realistic model parameters with  $\lambda_2 = 0.03125$ ,  $\lambda_1 = -4.37 \cdot 10^{-26}$  and time dependent temperature  $T(t)$  (5.4). In Figure 13 we show plot of the shape of  $V_{\phi_1}(t)$  for different time of evolution. It is easy to see that the phase transition associated with EWSB in tested model is of the second order.

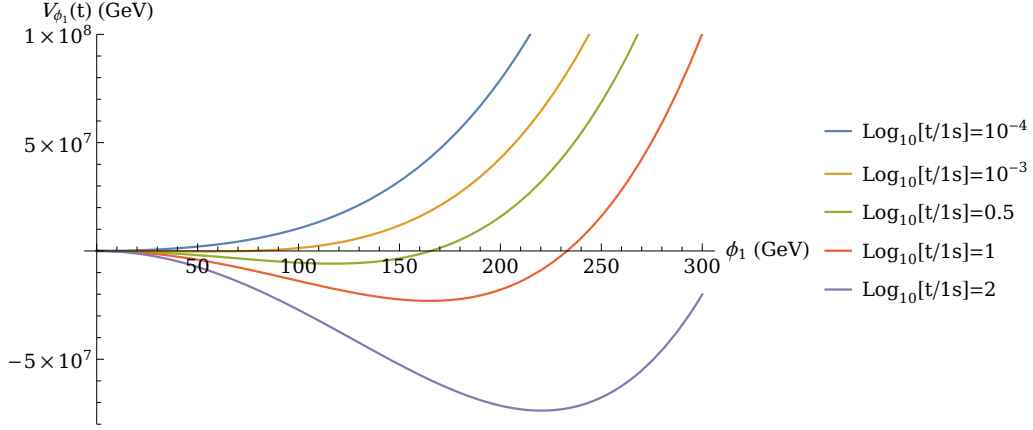


**Figure 13:** Plot of the potential for Higgs neutral component  $V_{\phi_1}(t)$  for different time values during evolution in hot Universe.

## 6 Additional scalars

Parameter space obtained from fulfilling numerical conditions on mass scales  $m_H^2$ ,  $v^2$  and  $M_P^2$  is rather constrained. One can relax these constraints by adding more scalar singlets to the model. Here we consider briefly addition of one more scalar singlet for simplicity. Then low energy Lagrangian density will take the form

$$\frac{\mathcal{L}_{mod}}{\sqrt{g}} = -\frac{1}{12}(\xi_0\phi_0^2 + \xi_1\phi_1^2 + \xi_2\phi_2^2)R + \sum_{i=0}^2 \frac{1}{2}\partial_\mu\phi_i\partial^\mu\phi_i - V_{mod}(\phi_0, \phi_1, \phi_2), \quad (6.1)$$

where potential  $V_{mod}$  is assumed to be

$$V_{mod}(\phi_0, \phi_1, \phi_2) = \lambda_0\phi_0^4 + \lambda_1\phi_0^2\phi_1^2 + \lambda_2\phi_1^4 + \lambda_3\phi_1^2\phi_2^2 + \lambda_4\phi_2^4, \quad (6.2)$$

so the new scalar  $\phi_2$  doesn't couple directly to the dilaton. Such a structure could be justified for instance by the locality of couplings in extra dimensions (space-time or internal). Taking  $\lambda_2$  and  $\lambda_4$  order one while  $\lambda_1, \lambda_3 \ll 1$ , one can easily arrange for a ground state displaying a hierarchy of vevs:

$$\langle\phi_0^2\rangle \gg \langle\phi_1^2\rangle \gg \langle\phi_2^2\rangle \quad (6.3)$$

and zero cosmological constant condition:

$$V_{mod}(\langle\phi_0\rangle, \langle\phi_2\rangle, \langle\phi_2\rangle) = 0, \quad (6.4)$$

where the explicit solution reads:

$$\langle\phi_1^2\rangle = \frac{2\lambda_1\lambda_4}{\lambda_3^2 - 4\lambda_2\lambda_4}\langle\phi_0^2\rangle, \quad \langle\phi_2^2\rangle = -\frac{\lambda_3}{2\lambda_4}\langle\phi_1^2\rangle = -\frac{\lambda_1\lambda_3}{\lambda_3^2 - 4\lambda_2\lambda_4}\langle\phi_0^2\rangle, \quad \lambda_0 = \frac{\lambda_1^2\lambda_4}{4\lambda_2\lambda_4 - \lambda_3^2}. \quad (6.5)$$

Then the effective Planck mass may become almost independent from the field playing the role of the Higgs and assuming the smallest vev:

$$M_P^2 \sim \xi_0\phi_0^2 + \xi_1\phi_1^2. \quad (6.6)$$

Such an extension of the scalar sector would allow building additional hierarchy of scales, while the thermal evolution for each pair of coupled scalars may follow approximately the scenario outlined above, this leading to the physically acceptable final state.

## 7 Summary and discussion

In this note we have analyzed the possible thermal corrections to the cosmological evolution of the scale symmetric scalar sector extending the standard Higgs sector. All sources of the explicit breaking of scale invariance other than the temperature corrections have been neglected. Eventual hierarchy of generated mass scales relies on a hierarchy of small couplings, which stays perturbatively stable. We have visualized the effects of the breaking of the scale symmetry by the thermal corrections and argued, that the dynamical restoration of the scale symmetry at low energies and late times due to thermal corrections dragging the expectation value of the dilaton towards the origin can be avoided in realistic physical models. We have also demonstrated with specific examples that starting with the acceptable initial conditions one can reach the physically relevant vacuum configuration as the result of the evolution of the scale symmetric scalar sector in the hot universe.

## Acknowledgments

This work has been supported by the Polish National Science Center grant 2017/27/B/ST2/02531.

## References

- [1] D. M. Ghilencea, “Manifestly scale-invariant regularisation and quantum effective operators,” *Phys. Rev. D* **93** (2016) no.10, 105006 doi:10.1103/PhysRevD.93.105006 [arXiv:1508.00595 [hep-ph]].
- [2] D. M. Ghilencea, “One-loop potential with scale invariance and effective operators,” *PoS CORFU2015* (2016), 040 doi:10.22323/1.263.0040 [arXiv:1605.05632 [hep-ph]].
- [3] D. M. Ghilencea, Z. Lalak and P. Olszewski, “Two-loop scale-invariant scalar potential and quantum effective operators,” *Eur. Phys. J. C* **76** (2016) no.12, 656 doi:10.1140/epjc/s10052-016-4475-0 [arXiv:1608.05336 [hep-th]].

- [4] D. M. Ghilencea, Z. Lalak and P. Olszewski, “Standard Model with spontaneously broken quantum scale invariance,” *Phys. Rev. D* **96** (2017) no.5, 055034 doi:10.1103/PhysRevD.96.055034 [arXiv:1612.09120 [hep-ph]].
- [5] D. M. Ghilencea, “Quantum implications of a scale invariant regularization,” *Phys. Rev. D* **97** (2018) no.7, 075015 doi:10.1103/PhysRevD.97.075015 [arXiv:1712.06024 [hep-th]].
- [6] D. M. Ghilencea and H. M. Lee, “Weyl gauge symmetry and its spontaneous breaking in the standard model and inflation,” *Phys. Rev. D* **99** (2019) no.11, 115007 doi:10.1103/PhysRevD.99.115007 [arXiv:1809.09174 [hep-th]].
- [7] D. M. Ghilencea, “Spontaneous breaking of Weyl quadratic gravity to Einstein action and Higgs potential,” *JHEP* **03** (2019), 049 doi:10.1007/JHEP03(2019)049 [arXiv:1812.08613 [hep-th]].
- [8] D. M. Ghilencea, “Stueckelberg breaking of Weyl conformal geometry and applications to gravity,” *Phys. Rev. D* **101** (2020) no.4, 045010 doi:10.1103/PhysRevD.101.045010 [arXiv:1904.06596 [hep-th]].
- [9] D. M. Ghilencea, “Weyl  $R^2$  inflation with an emergent Planck scale,” *JHEP* **10** (2019), 209 doi:10.1007/JHEP10(2019)209 [arXiv:1906.11572 [gr-qc]].
- [10] D. M. Ghilencea, “Gauging scale symmetry and inflation: Weyl versus Palatini gravity,” *Eur. Phys. J. C* **81** (2021) no.6, 510 doi:10.1140/epjc/s10052-021-09226-1 [arXiv:2007.14733 [hep-th]].
- [11] D. M. Ghilencea, “Standard Model in Weyl conformal geometry,” *Eur. Phys. J. C* **82** (2022) no.1, 23 doi:10.1140/epjc/s10052-021-09887-y [arXiv:2104.15118 [hep-ph]].
- [12] D. M. Ghilencea and T. Harko, “Cosmological evolution in Weyl conformal geometry,” [arXiv:2110.07056 [gr-qc]].
- [13] D. M. Ghilencea, “Non-metricity as the origin of mass generation in gauge theories of scale invariance,” [arXiv:2203.05381 [hep-th]].
- [14] Z. Lalak and P. Olszewski, “Vanishing trace anomaly in flat spacetime,” *Phys. Rev. D* **98** (2018) no.8, 085001 doi:10.1103/PhysRevD.98.085001 [arXiv:1807.09296 [hep-th]].
- [15] Coleman Weinberg radiative corrections...
- [16] <https://pdg.lbl.gov/2018/reviews/rpp2018-rev-kinematics.pdf>
- [17] F. D’Eramo, R. Z. Ferreira, A. Notari and J. L. Bernal, “Hot Axions and the  $H_0$  tension,” *JCAP* **11** (2018), 014 doi:10.1088/1475-7516/2018/11/014 [arXiv:1808.07430 [hep-ph]].
- [18] M. Sher, “Electroweak Higgs Potentials and Vacuum Stability,” *Phys. Rept.* **179** (1989), 273-418 doi:10.1016/0370-1573(89)90061-6
- [19] M. E. Carrington, “The Effective potential at finite temperature in the Standard Model,” *Phys. Rev. D* **45** (1992), 2933-2944 doi:10.1103/PhysRevD.45.2933
- [20] M. Quiros, “Finite temperature field theory and phase transitions,” [arXiv:hep-ph/9901312 [hep-ph]].
- [21] A. Megevand and A. D. Sanchez, “Supercooling and phase coexistence in cosmological phase transitions,” *Phys. Rev. D* **77** (2008), 063519 doi:10.1103/PhysRevD.77.063519 [arXiv:0712.1031 [hep-ph]].
- [22] L. Husdal, “On Effective Degrees of Freedom in the Early Universe,” *Galaxies* **4** (2016) no.4, 78 doi:10.3390/galaxies4040078 [arXiv:1609.04979 [astro-ph.CO]].

- [23] M. Heikinheimo, A. Racioppi, M. Raidal, C. Spethmann and K. Tuominen, “Physical Naturalness and Dynamical Breaking of Classical Scale Invariance,” *Mod. Phys. Lett. A* **29** (2014), 1450077 doi:10.1142/S0217732314500771 [arXiv:1304.7006 [hep-ph]].
- [24] K. Kannike, A. Racioppi and M. Raidal, “Embedding inflation into the Standard Model - more evidence for classical scale invariance,” *JHEP* **06** (2014), 154 doi:10.1007/JHEP06(2014)154 [arXiv:1405.3987 [hep-ph]].
- [25] K. Kannike, G. Hütsi, L. Pizza, A. Racioppi, M. Raidal, A. Salvio and A. Strumia, “Dynamically Induced Planck Scale and Inflation,” *PoS EPS-HEP2015* (2015), 379 doi:10.22323/1.234.0379
- [26] K. Kannike, M. Raidal, C. Spethmann and H. Veermäe, “The evolving Planck mass in classically scale-invariant theories,” *JHEP* **04** (2017), 026 doi:10.1007/JHEP04(2017)026 [arXiv:1610.06571 [hep-ph]].
- [27] K. Kannike, N. Koivunen, A. Kubarski, L. Marzola, M. Raidal, A. Strumia and V. Vipp, “Dark matter-induced multi-phase dynamical symmetry breaking,” *Phys. Lett. B* **832** (2022), 137214 doi:10.1016/j.physletb.2022.137214 [arXiv:2204.01744 [hep-ph]].
- [28] M. Shaposhnikov and D. Zenhausern, “Scale invariance, unimodular gravity and dark energy,” *Phys. Lett. B* **671** (2009), 187-192 doi:10.1016/j.physletb.2008.11.054 [arXiv:0809.3395 [hep-th]].
- [29] M. Shaposhnikov and D. Zenhausern, “Quantum scale invariance, cosmological constant and hierarchy problem,” *Phys. Lett. B* **671** (2009), 162-166 doi:10.1016/j.physletb.2008.11.041 [arXiv:0809.3406 [hep-th]].
- [30] J. Garcia-Bellido, J. Rubio, M. Shaposhnikov and D. Zenhausern, “Higgs-Dilaton Cosmology: From the Early to the Late Universe,” *Phys. Rev. D* **84** (2011), 123504 doi:10.1103/PhysRevD.84.123504 [arXiv:1107.2163 [hep-ph]].
- [31] M. Shaposhnikov, A. Shkerin, I. Timiryasov and S. Zell, “Einstein-Cartan gravity, matter, and scale-invariant generalization ,” *JHEP* **10** (2020), 177 doi:10.1007/JHEP08(2021)162 [arXiv:2007.16158 [hep-th]].
- [32] G. K. Karananas, M. Shaposhnikov, A. Shkerin and S. Zell, “Scale and Weyl invariance in Einstein-Cartan gravity,” *Phys. Rev. D* **104** (2021) no.12, 124014 doi:10.1103/PhysRevD.104.124014 [arXiv:2108.05897 [hep-th]].
- [33] M. Shaposhnikov and A. Tokareva, “Anomaly-free scale symmetry and gravity,” [arXiv:2201.09232 [hep-th]].
- [34] P. G. Ferreira, C. T. Hill and G. G. Ross, “Scale-Independent Inflation and Hierarchy Generation,” *Phys. Lett. B* **763** (2016), 174-178 doi:10.1016/j.physletb.2016.10.036 [arXiv:1603.05983 [hep-th]].
- [35] P. G. Ferreira, C. T. Hill and G. G. Ross, “Weyl Current, Scale-Invariant Inflation and Planck Scale Generation,” *Phys. Rev. D* **95** (2017) no.4, 043507 doi:10.1103/PhysRevD.95.043507 [arXiv:1610.09243 [hep-th]].
- [36] P. G. Ferreira, C. T. Hill, J. Noller and G. G. Ross, “Inflation in a scale invariant universe,” *Phys. Rev. D* **97** (2018) no.12, 123516 doi:10.1103/PhysRevD.97.123516 [arXiv:1802.06069 [astro-ph.CO]].
- [37] P. G. Ferreira, C. T. Hill, J. Noller and G. G. Ross, “Scale-independent  $R^2$  inflation,” *Phys.*



Rev. D **100** (2019) no.12, 123516 doi:10.1103/PhysRevD.100.123516 [arXiv:1906.03415 [gr-qc]].